Bioresource Technology 258 (2018) 158–167

Contents lists available at ScienceDirect

Bioresource Technology

journal homepage: www.elsevier.com/locate/biortech

Hydrothermal liquefaction of high- and low-lipid algae: Mass and energy balances

Feng Cheng[a], Zheng Cui[a], Kwonit Mallick[a], Nagamany Nirmalakhandan[b], Catherine E. Brewer[a,*]

[a] Department of Chemical and Materials Engineering, New Mexico State University, P.O. Box 30001 MSC 3805, Las Cruces, NM 88003, USA
[b] Department of Civil Engineering, New Mexico State University, P.O. Box 30001 MSC 3CE, Las Cruces, NM 88003, USA

GRAPHICAL ABSTRACT

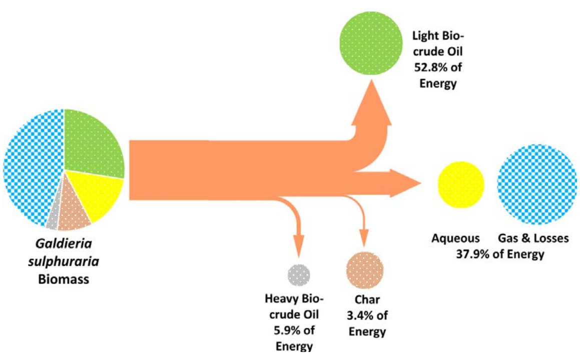

ARTICLE INFO

Keywords:
Hydrothermal liquefaction
Bio-crude oil
High protein algae
Mass balance
Energy balance

ABSTRACT

Hydrothermal liquefaction (HTL) of high-lipid microalgae *Nannochloropsis salina* (*N. salina*) and low-lipid microalgae *Galdieria sulphuraria* (*G. sulphuraria*) were run under subcritical conditions (310–350 °C and 10–17 MPa) in a 1.8 L batch autoclave system. HTL mass and energy balances for both species were compared under different operating conditions to predict the optimum reaction conditions for new algae strains based on their feedstock composition. Bio-crude oils and chars were characterized by bomb calorimetry, elemental analysis, inductively coupled plasma optical emission spectrometry (ICP-OES), and thermogravimetric analysis (TGA). Under the optimized conditions, 59 wt% and 31 wt% bio-crude oil yields were obtained from HTL of *N. salina* and *G. sulphuraria*, while 85% and 59% of the feedstock energy were partitioned into *N. salina*-derived and *G. sulphuraria*-derived bio-crude oils, respectively. More favorable energy balances were related to shorter reaction times and higher algal solid contents.

1. Introduction

Third-generation biofuels produced from hydrothermal liquefaction (HTL) of algae have been developing rapidly. The main advantages of algae-derived oils via HTL include high algae growth rates, strong CO_2-mitigation potential, and avoidance of feedstock drying requirements. The effect of algal composition on the yields of bio-crude oil from HTL has been frequently studied in the last decade (Barreiro et al., 2013). In general, the higher the lipid content in the algae biomass, the higher the yield of bio-crude oil (Biddy et al., 2013); past work has demonstrated bio-crude yields of 30–60 wt%, with the energy recoveries (ratio of energy content in the bio-crude oil to energy content in the feedstock) of 50–70%. A kinetic study (Valdez et al., 2014) suggested that lipid- and protein-rich algae could produce higher yields of bio-crude oil than

* Corresponding author.
E-mail address: cbrewer@nmsu.edu (C.E. Brewer).

https://doi.org/10.1016/j.biortech.2018.02.100
Received 22 December 2017; Received in revised form 21 February 2018; Accepted 22 February 2018
Available online 24 February 2018
0960-8524/

carbohydrate-rich algae. Similarly, Chakraborty et al. (Chakraborty et al., 2012) observed that the yield of bio-crude oil was hardly impacted when the carbohydrates were extracted from the algal biomass prior to HTL, while the yield of char was substantially reduced. This demonstrates that much of the char fraction is carbohydrate-derived and much of the oil fraction is lipid- and protein-derived.

In this study, HTL of two algal species, high-lipid microalgae *Nannochloropsis salina* and low-lipid microalgae *G. sulphuraria*, were compared to investigate the HTL performance of *G. sulphuraria* as a promising candidate for wastewater treatment with energy recovery.

Nannochloropsis is a marine genus of microalgae that is an outstanding candidate for biofuel production due to its high lipid content (up to 30 wt%) and biomass productivity (up to $0.2\,g\,L^{-1}\,day^{-1}$) (Rodolfi et al., 2009). HTL of *Nannochloropsis* sp. achieved a bio-crude oil yield of 43 wt% at 350 °C and 60 min (Brown et al., 2010).

Galdieria sulphuraria is a mixotrophic microalgae able to grow at temperatures from 25 to 55 °C (Toplin et al., 2008). Its tolerance of acidic conditions and higher temperatures make *G. sulphuraria* promising for outdoor algal cultivation since the ponds require less cooling and few invasive species can survive the conditions. These advantages lead to lower energy consumption and lower costs for cultivation compared to other species of microalgae (Chen et al., 2002). *G. sulphuraria* has a high salt and metal tolerance (Schönknecht et al., 2013), and can grow on a wide range of organic substrates (Reeb and Bhattacharya, 2010). Recently, the ability of *G. sulphuraria* for eliminating biological oxygen demand (BOD), nitrogen, and phosphorous from primary-settled wastewater has been demonstrated (Selvaratnam et al., 2015a), indicating the potential for using *G. sulphuraria* to treat wastewater and prevent eutrophication (Chen et al., 2002). The few results currently available on HTL of *G. sulphuraria* suggest that bio-crude oil yields are relatively low: < 22 wt% (Selvaratnam et al., 2015b).

Most studies on HTL of microalgae have used lab-scale batch reactors (4–2000 mL) (Jena et al., 2011). To commercialize HTL processes, continuous HTL reactors need to be developed. In continuous reactors, bio-crude oils have the advantage of being obtained by gravity separation rather than organic solvent extraction (Elliott et al., 2013b). Solvent extraction usually reduces the quality of bio-crude oil by incorporating water-soluble heteroatom-rich components (Barreiro et al., 2015a,; Xu and Savage, 2014). Continuous reactors can achieve higher heating rates and shorter residence times, which favor bio-crude oil production (Biller et al., 2015). Economically feasible continuous HTL processes for algae have been proposed (Elliott et al., 2013a; Jazrawi et al., 2013). These processes incorporate plug-flow tubular reactors in which high-pressure cylinder filters remove char from the HTL product flow, allowing longer operating times (Elliott et al., 2013b). Since 2015, several other continuous HTL reactors have been reported for processing of algae (Barreiro et al., 2015b,; Biller et al., 2015), but persistent clogging issues in filters and pumps has prevented long-term continuous operation to date (Barreiro et al., 2015b). To make the transition to continuous flow systems, better understanding of the chemical and physical properties of feedstocks and products is necessary. Batch reaction studies and feedstock/char characterization can help provide this information.

The objectives of this study were to: 1) quantify the mass and energy balances associated with HTL of the low-lipid species, *G. sulphuraria,* under varying reaction conditions using a larger (1.8 L) batch reactor, 2) compare HTL of *G. sulphuraria* with HTL of a high-lipid species, *N. salina,* and 3) provide recommendations regarding solids loadings and reaction conditions for HTL conversion of these species in continuous flow reactors.

2. Materials and methods

2.1. Algae production and harvesting

A starter culture of *Nannochloropsis salina* (CCMP1776) was obtained from the Provasoli-Guillard National Center for Culture of Marine Phytoplankton (CCMP). The starter culture was expanded in 20 L carboys prior to being transferred to an outdoor photo bioreactor system (Solix Algredients, Fort Collins, CO), located at the NMSU Algal Growth Facility at the Fabian Garcia Science Center, Las Cruces, NM. The algae were grown in 200 L batch cultures in f/2 growth medium with 2% ocean salts (Cheng et al., 2017). *Galdieria sulphuraria* (CCMEE 5778.1) was identified by the Culture Collection of Microorganisms from Extreme Environments (University of Oregon). The strain was grown in a modified cyanidium medium with the pH adjusted to 2.5 (Cheng et al., 2017). The algae were grown in the outdoor photobioreactor system located at the NMSU Algal Growth Facility using natural photoperiod and light intensity. The temperature in the enclosed growth bags was substantially hotter than the ambient air temperature. Algal cultures were harvested and concentrated by a custom-built high-speed continuous centrifuge (AC26VHC, Type 265322CD, Pennwalt, India) at 15,000 rpm for 1–2 h with a flow rate of 8 L/min. Samples were stored at −20 °C prior to analysis and conversion.

2.2. Hydrothermal liquefaction and product recovery

HTL experiments were performed in a 1.8 L Model 4572 stainless steel batch reactor with a Model 4848B controller unit (Parr Instrument Co., Moline, IL). Algae slurries at two different solids loadings (5 and 10 wt%) were converted at temperatures of 310, 330 and 350 °C and reaction times of 5, 30 and 60 min, as shown in Table 2. For each experiment, 500 mL of algae slurry was prepared by mixing desired amounts of solid algae with deionized water. The reactor was pressurized to approximately 1.4 MPa before starting the heating program. The slurry was stirred with an impeller throughout the reaction. Once the reaction was complete, the reactor was cooled to room temperature with the tap water cooling jacket and the off gas was vented into a fume hood to reduce the pressure back to atmospheric.

The HTL products were recovered by adding 200 mL of hexane into the reactor to extract volatile organics from the aqueous phase into the oil phase. Three additional aliquots (150 mL) of hexane were used to rinse the reactor and the rinseates were added to the product mixture. The product mixture was vacuum filtered through Whatman® No. 4 filter paper (pore size = 20–25 μm), then Whatman® No. 1 filter paper (pore size = 11 μm) to collect the solid products: an asphalt-like sticky black residue, char, and yellowish ash powders. The hexane-soluble product, designated as light bio-crude oil (LBO), was separated from the aqueous phase using a separatory funnel. The solid residues on the filter paper were rinsed using 75 mL dichloromethane (DCM) and filtered again. The DCM-soluble, hexane-insoluble organic product was designated as heavy bio-crude oil (HBO). The solvents were removed from the oils by vacuum evaporation at 40–50 °C using a rotary evaporator. The aqueous phase, LBO, and HBO were stored at 4 °C prior to analysis. Solid residues were dried at 65 °C overnight in a drying oven and designated as biosolid/char. The remaining mass fraction was designated as gases and losses. Yields of HTL products were calculated on a dry algal biomass basis (Cheng et al. 2017). To simplify the analysis of HTL yields in terms of different reaction conditions, temperature and reaction time are combined into one variable, the reaction ordinate (Overend et al., 1987). A reaction ordinate equation, modified to account for a more gradual HTL heating rate, was used here, as described in (Cheng et al., 2017).

2.3. Characterization of feedstocks and HTL products

Higher heating values (HHV) of the algal feedstocks and HTL

Table 1
Elemental analysis for feedstock and light (hexane-soluble) bio-crude oils from HTL of *N. salina* and *G. sulphuraria* under different operating conditions on a dry weight basis. Log R_t = logarithmic reaction ordinate.

Solid Algal Content wt%	Temp. °C	Time min	Log (R_t)	Elemental analysis wt%							
				C	H	N	S	O[a]	H/C	O/C	N/C
G. sulphuraria CCMEE 5587.1 feedstock				44.5 ± 0.2	7.3 ± 1.7	9.5 ± 0.2	3.0 ± 0.6	25.4 ± 1.9	1.95	0.43	0.18
5	310	60	8.03	78.1 ± 2.1	10.7 ± 0.2	5.8 ± 0.6	2.9 ± 0.2	2.6 ± 2.2	1.63	0.02	0.06
5	350	5	8.55	78.9 ± 0.3	10.4 ± 0.2	5.4 ± 0.6	3.4 ± 0.1	1.9 ± 0.6	1.57	0.02	0.06
5	330	60	8.62	75.8 ± 1.1	10.2 ± 0.4	6.1 ± 0.4	3.1 ± 0.0	4.9 ± 1.2	1.60	0.05	0.07
5	350	30	8.97	74.3 ± 0.3	10.2 ± 0.1	6.7 ± 1.4	3.1 ± 0.0	5.7 ± 1.4	1.63	0.06	0.08
5	350	60	9.21	79.8 ± 0.7	10.5 ± 0.1	4.5 ± 0.7	3.2 ± 0.1	2.0 ± 1.0	1.57	0.02	0.05
10	350	60	9.21	76.5 ± 0.8	10.0 ± 0.3	6.6 ± 0.3	3.6 ± 0.1	3.3 ± 0.9	1.56	0.03	0.07
N. salina CCMP 1776 feedstock				55.9 ± 0.3	7.9 ± 0.3	2.9 ± 0.3	2.8 ± 0.2	23.3 ± 0.7	1.67	0.31	0.04
5	310	5	7.35	75.9 ± 2.6	11.7 ± 0.3	3.0 ± 0.4	2.3 ± 0.3	7.1 ± 2.7	1.84	0.07	0.03
5	310	30	7.78	75.5 ± 0.7	11.8 ± 0.3	2.6 ± 0.3	2.3 ± 0.2	7.8 ± 0.9	1.86	0.08	0.03
5	310	60	8.03	76.0 ± 0.1	11.4 ± 0.8	2.4 ± 0.1	2.2 ± 0.0	8.2 ± 1.1	1.75	0.08	0.03
10	310	60	8.03	76.4 ± 1.4	11.4 ± 0.3	3.1 ± 0.6	2.1 ± 0.3	7.0 ± 1.6	1.79	0.07	0.04
5	330	60	8.62	76.5 ± 0.5	11.9 ± 0.1	2.7 ± 0.2	2.1 ± 0.2	6.8 ± 0.6	1.86	0.07	0.03
5	350	60	9.21	75.8 ± 0.5	11.5 ± 0.3	3.5 ± 0.2	2.5 ± 0.4	6.8 ± 0.8	1.81	0.07	0.04

[a] By difference.

products were determined using a Model 6725 semi-micro bomb calorimeter (Parr Instrument Company, Moline, IL). Samples (20–30 mg) were analyzed in at least duplicate. Elemental CHNS content was measured using a Series II 2400 elemental analyzer (Perkin Elmer, Waltham, MA). Samples were analyzed in duplicate or triplicate depending on the amount of sample available. Thermogravimetric analysis (TGA) of lyophilized algal feedstock and LBO samples (15 ± 2 mg, dry basis) was carried out on a thermogravimetric analyzer (TGA-Q500, TA Instruments, New Castle, DE) using platinum pans. Samples were heated from room temperature to 800 °C at 10 °C/min under N_2 (60 mL/min). Lipid, carbohydrate, protein, and ash contents of the algae biomass were measured by the standard methods developed by the National Renewable Energy Laboratory (Hames et al., 2008; Wychen and Laurens, 2013a; Wychen and Laurens, 2013b; Wychen et al., 2013). Moisture contents of algal biomass and aqueous samples were measured in triplicate using a FreeZone 12 L Console Freeze Dry System with Stoppering Tray Dryer (Labconco, Kansas City, MO). Particle size and shape of the *G. sulphuraria* cells were characterized using a FlowCAM flow cytometer (Fluid Imaging Technologies, Yarmouth, ME) at a flow rate of 0.03 mL/min and an image collection rate of 0.68 frames/s. Total organic carbon (TOC) of the aqueous phase products was measured using a model TOC-V_{CPH} analyzer (Shimadzu Corp., Kyoto, Japan). Aqueous phase pH and electrical conductivity were measured with a benchtop combination meter. To measure the materials' inorganic composition, algal biomass, bio-crude oil, and char samples (0.2 g) were digested with 30% HCl (6 mL) and 70% HNO_3 (6 mL) in a Multiwave 3000 microwave digestion system (Anton Paar, Ashland, VA). Digestates were diluted to 100 mL with deionized (DI) water and the elements quantified using an Optima 4300 DV inductively coupled plasma optical emission spectrophotometer (ICP-OES) (PerkinElmer, Waltham, MA).

2.4. Evaluation of energy recovery

Energy recovery (ER) for hydrothermal liquefaction was calculated by:

$$\mathrm{ER} = \frac{\text{Energy available from LBO}}{\text{Energy available from algae}} = \frac{\text{Mass of LBO} \times \text{HHV of LBO}}{\text{Mass of dry algae} \times \text{HHV of dry algae}} \times 100\% \quad (1)$$

where LBO is the hexane-soluble bio-crude oil and HHV is the higher heating value (dry basis) obtained by bomb calorimetry. The energy consumption ratio (ECR), the ratio of the energy required for conversion of algae into bio-crude oil to the energy available from bio-crude oil combustion, was calculated as:

$$\mathrm{ECR} = \frac{[R_w \times C_{pw} + (1-R_w) \times C_{ps}] \times (T-T_0) \times (1-r_2)}{(1-R_w) \times R_0 \times Y \times \mathrm{HHV} \times r_1} \times 100\% \quad (2)$$

where R_W is the moisture content, C_{pw} and C_{ps} are the average specific heats of water and dry algal biomass, respectively, T is the reaction temperature, T_{00} is the starting temperature before the reaction, R_0 is the organic matter content (dry basis), Y is the oil yield, HHV is the higher heating value of the oil, r_1 is the efficiency of the combustion process, and r_2 is the efficiency of heat recovery. Here, the values assumed were $C_{pw} = 4.18\ \mathrm{kJ\,kg^{-1}\,K^{-1}}$, $C_{ps} = 1.25\ \mathrm{kJ\,kg^{-1}\,K^{-1}}$ (Minowa et al., 1995), $r_1 = 0.6$, and $r_2 = 0.5$ (Minowa et al., 1998). Lower ECR values are desirable; values of ECR > 1 indicate that more energy was used to perform the conversion than was available in the products if combusted.

2.5. Statistical analysis

Results were analyzed by factorial analysis of one-way variance (ANOVA) using SPSS 17 software. Duncan's multiple range test was used to compare the means of HTL product yields under different operating conditions, at a significance level of $p < 0.05$.

3. Results and discussion

3.1. Feedstock characteristics

Feedstock characteristics for *N. salina* were: 28.5 wt% solids loading (wet basis), 7.3 wt% ash (dry basis), 27.0 MJ/kg HHV (dry basis), and 19.7, 13.5, 22.9 wt% lipid, protein, and carbohydrate, respectively (dry, ash-free basis). Feedstock characteristics for *G. sulphuraria* were: 31.0 wt% solids loading (wet basis), 10.4 wt% ash (dry basis), 20.5 MJ/kg HHV (dry basis), and 5.5, 45.3, 14.5 wt% lipid, protein, and carbohydrate, respectively (dry, ash-free basis) (Cheng et al., 2017). CHNS of the two algae are shown in Table 1. *N. salina* contains less ash and three times as much lipid content as *G. sulphuraria,* leading to a higher carbon content. The oxygen content of *N. salina* is slightly lower than that of *G. sulphuraria* even though it has much more carbohydrate. *G. sulphuraria* contains almost three times as much protein as *N. salina*, resulting in a much higher nitrogen content and N/C ratio. The cellular components not quantified here include phosphorous-containing compounds (from lipid head groups and nucleic acids), un-extracted sugar derivatives (i.e. uronic acids and amino sugars), un-extracted pigments (i.e. beta

Table 2
HTL product distributions of *N. salina* and *G. sulphuraria* under different operating conditions. Range indicates standard deviation where n = 2 or 3. LBO = light (hexane-soluble) bio-crude oil; HBO = heavy (hexane-insoluble, DCM-soluble) bio-crude oil, Log R_t = logarithmic reaction ordinate.

Solid Algal Content wt% [a]	Temp. °C	Time min	Log (R_t)	LBO Yield wt%[a]	HBO Yield wt%[a]	Char Yield wt%[a]	Aqueous Phase Yield wt%[a]	Gas Yield and Loss wt%[a]
G. sulphuraria CCMEE 5587.1								
5	310	60	8.03	18.1 ± 1.2[b]	5.0 ± 1.1[bc]	13.0 ± 2.0[d]	36.5 ± 1.8[d]	27.4 ± 0.3[e]
5	350	5	8.55	20.1 ± 0.8[bcd]	8.9 ± 0.6[cde]	9.4 ± 0.8[c]	19.8 ± 0.4[b]	41.9 ± 0.2[f]
5	330	60	8.62	19.6 ± 1.0[bc]	6.1 ± 0.4[bcde]	9.7 ± 1.9[c]	26.0 ± 4.7[c]	38.7 ± 1.4[f]
5	350	30	8.97	22.6 ± 2.7[d]	8.4 ± 2.0[cde]	9.7 ± 0.6[c]	17.4 ± 6.0[b]	42.0 ± 7.3[f]
5	350	60	9.21	27.5 ± 0.7[e]	3.3 ± 2.4[b]	9.4 ± 0.7[c]	14.9 ± 1.4[b]	45.0 ± 1.0[f]
10	350	60	9.21	21.7 ± 0.2[cd]	9.7 ± 1.5[e]	9.7 ± 1.5[c]	13.7 ± 0.2[b]	45.1 ± 3.3[f]
N. salina CCMP 1776								
5	310	5	7.35	49.6 ± 1.0[g]	9.4 ± 4.2[de]	6.1 ± 1.0[b]	26.5 ± 3.6[c]	8.4 ± 1.5[b]
5	310	30	7.78	51.8 ± 0.2[gh]	5.4 ± 0.0[bcd]	5.5 ± 0.7[b]	26.3 ± 0.4[c]	10.9 ± 0.9[bc]
5	310	60	8.03	54.3 ± 1.5[h]	4.8 ± 1.4[bc]	4.3 ± 1.2[b]	19.1 ± 4.2[b]	17.5 ± 5.3[cd]
10	310	60	8.03	52.4 ± 0.6[gh]	2.8 ± 0.5[b]	9.8 ± 1.8[c]	19.1 ± 1.9[b]	15.9 ± 3.6[bcd]
5	330	60	8.62	52.8 ± 1.7[h]	3.7 ± 1.3[b]	4.8 ± 1.7[b]	16.4 ± 0.5[b]	22.4 ± 4.3[de]
5	350	60	9.21	40.0 ± 1.3[f]	3.9 ± 1.1[b]	4.8 ± 1.3[b]	13.4 ± 2.1[b]	37.9 ± 1.6[f]

[b–h]Different superscripts within the same column indicate significant differences between the means at $p < 0.05$ by Duncan's multiple range test.
[a] Dry feedstock basis.

carotene), some membrane proteins, algaenan (i.e. isoprenoids) (Simpson et al., 2003), and other elements.

For the 33,419 *G. sulphuraria* particles counted, the minimum, maximum, and mean diameters were 2.3 µm, 61.1 µm, and 8.86 µm, respectively. The D10, D25, D50, D75 and D90 diameter fractions were 3.39, 4.24, 6.14, 10.39 and 17.96 µm, respectively, indicating that most of the cells had diameters within a relatively narrow range between 4 and 10 µm with a few larger cells (and probably clumps of cells). Previous measurements indicated that *N. salina* cells are smaller, ranging from 2 µm to 3.9 µm (Campos et al., 2014; Chretiennot-Dinet et al., 1991). Proper agitation in continuous feed systems will be needed to prevent the algae cells from settling and aggregating into larger clumps, which may lead to deposits and clogs.

3.2. HTL product yields

LBO yields for both algae species show statistically significant changes under different operating conditions. LBO and combined bio-crude oil yields (LBO + HBO) were much higher for *N. salina* (40–54 wt% and 44–59 wt%, respectively) than for *G. sulphuraria* (18–27 wt% and 23–31 wt%, respectively) (Cheng et al., 2017). For *N. salina*, the LBO yields decreased with temperature and increased with reaction time, while LBO yields for *G. sulphuraria* increased with both temperature and reaction time. The increase in yields at higher temperatures is attributed to the conversion of proteins and carbohydrates into low-polarity heterocyclic compounds via Maillard, amidation, esterification, and rearrangement reactions. Lipid-derived molecules are converted into the HTL organic phase by hydrolysis at much lower temperatures (< 180 °C) (Sudasinghe et al., 2015). Higher temperatures favor decomposition to gases and repolymerization reactions to heavy bio-crude oil for lipid-derived molecules, which decreases LBO yields.

HBO yields for both species decreased with increasing reaction time. HBO represented a higher fraction of the total bio-crude recovery for *G. sulphuraria* (11–31%) compared to that of *N. salina* (5–16%) bio-crude oils, which is attributed to the higher amount of nitrogen-containing compounds derived from protein (Cheng et al., 2017). These heterocyclic poly-aromatic compounds can increase oil molecular weight, oil viscosity, formation of soot and particulate emissions (Richter and Howard, 2000), storage material corrosion (Hu et al., 2012), and difficulty in catalytic upgrading.

For both species, aqueous organic yields decreased and gas product yields increased with increasing temperature and/or reaction time (Table 2). Higher temperatures and longer reaction times convert protein-derived amino acids and carbohydrate-derived saccharides in the aqueous phase into the organic phase through hydrodeoxygenation, hydrodenitrogenation, and decarboxylation, which simultaneously generate more CO_2, NH_3, CH_4 and H_2 (Jena et al., 2011). Char yields remained almost unchanged with reaction conditions and reflect the ash content of the feedstock, being higher for *G. sulphuraria* than for *N. salina*. These product distributions are consistent with the literature and suggest that lower temperature should be used for high-lipid feedstocks while higher temperatures should be used for low-lipid feedstocks. Longer batch reaction times, up to 60 min tested here, favor LBO yields.

Various studies on HTL of *Nannochloropsis* and *Galdieria* species have been carried out in the last decade (Reddy et al., 2016; Selvaratnam et al., 2015b). The yield of bio-crude oil for *N. salina* (59 wt%) in this study is higher than most results reported (35–60 wt%) (Barreiro et al., 2013; Xu and Savage, 2014); the highest yield of bio-crude oil reported (66 wt%) was achieved using more intense reaction conditions (600 °C for 1 min, or R_t = 14.8) and much higher heating rates (Faeth et al., 2013). The reaction ordinate for producing the highest yield of bio-crude oil in this study is moderate (8.03) relative to those (7.2–9.2) from previous studies (Leow et al., 2015; Li et al., 2014). The yield of total bio-crude oil (LBO + HBO) observed for HTL of *G. sulphuraria* here are the highest reported to date (31.4 wt% compared to 22.3 wt%), however, the reaction conditions were more severe (with higher energy input requirements) (Selvaratnam et al., 2015b). One expected advantage of future conversion in a continuous flow reactor is that the higher heating rates (100–200 °C/min vs. approximately 3 °C/min in the batch reactor) will lead to further increases in oil yields (Biller et al., 2015).

3.3. Thermogravimetric analysis of algae biomass and light bio-crude oils

Weight loss curves of the algal biomass samples and LBOs obtained using thermogravimetric analysis (TGA) are shown in Figs. 1 and 2. Biomass from both species had little weight loss below 240 °C (approximately 7 wt%). *G. sulphuraria* biomass had a steeper weight loss slope than *N. salina* at 240–320 °C (42 wt% loss to 37 wt%, respectively) because the decomposition of the higher protein content; from 320 to 500 °C, *N. salina* biomass had the faster weight loss (37 wt% loss to 17 wt%, respectively) due to the decomposition of the higher amounts of lipids and carbohydrates (Wychen et al., 2013). *G. sulphuraria* produced more carbonaceous residue (> 540 °C) than *N. salina* (28 wt% vs. 19 wt%), suggesting *N. salina* is easier to convert into bio-crude oil, as would be expected from the LBO yields (Table 2).

From the differential thermogravimetric (DTG) curves of the bio-crude oils (Figs. 1 and 2), the highest peaks shifting towards lower

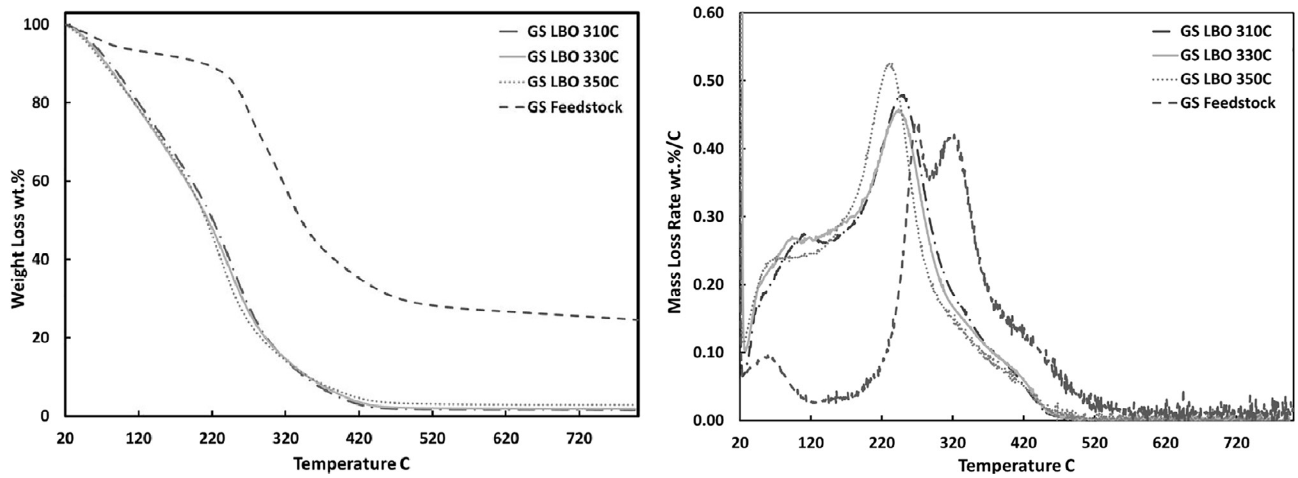

Fig. 1. Thermal decomposition/volatilization (left) and differential thermogravimetric (DTG) curves (right) of 5 wt% *G. sulphuraria* and light bio-crude oil (LBO) produced under different HTL temperatures and 60 min. GS = *G. sulphuraria*; numbers indicate HTL reaction temperature.

temperatures indicates that HTL at higher temperatures effectively broke cell structures into smaller molecules with lower volatilization temperatures. *G. sulphuraria* LBOs show broader DTG curves relative to those of *N. salina* LBOs (ranging from 60 to 340 °C vs. 140 to 300 °C), demonstrating the wider variety of volatile compounds in *G. sulphuraria* LBOs. In addition, volatilization temperatures of *G. sulphuraria* LBOs were less sensitive to HTL temperature compared to *N. salina* LBOs, due to the lower lipid content in *G. sulphuraria* (Reddy et al., 2016).

3.4. Elemental analysis and energy recovery in light bio-crude oil fraction

Table 1 shows the CHNS elemental contents and elemental ratios of the LBO fractions. Compared to algal feedstock, all LBO fractions contain more carbon (74–79 wt%) and hydrogen (10–12 wt%), and less oxygen (2–8 wt%) and nitrogen (2–7 wt%), suggesting aliphatic compounds were enriched, and biomass was deoxygenated and denitrogenated during HTL, as reported in (Tian et al., 2015). *G. sulphuraria*-derived LBO contained more nitrogen (4.5–6.7 wt% vs. 2.6–3.5 wt%) and higher N/C ratios, and less oxygen (1.9–5.7 wt% vs. 6.8–8.2 wt%) and lower O/C ratios than *N. salina*-derived LBO, due to *G. sulphuraria*'s higher protein and lower carbohydrate contents, respectively. For *G. sulphuraria*-derived LBO, more severe reaction conditions resulted in lower H/C, O/C, and N/C ratios. H/C ratios increased with reaction severity for *N. salina*-derived LBO, while no clear trends were seen for O/C and N/C ratios. More heteroatom-containing compounds in *G. sulphuraria* possessed unstable structures and were prone to desaturation during heating, while lipid-derived products with high H/C ratios were concentrated in *N. salina*-derived LBO (Cheng et al., 2017). LBO O/C and N/C ratios in this study, 0.02–0.08 and 0.03–0.05, respectively, were lower than those in previous studies (Biller and Ross, 2011; Faeth et al., 2013). The lower ratios of O/C and N/C may be related to the lower polarity of solvent used in bio-crude oil recovery (e.g. hexane). Nevertheless, upgrading is still needed to create oils with lower ratios of O/C and N/C comparable to those in petroleum-derived oils (O/C = 0.0004–0.01 and N/C = 0.001–0.02) (Speight, 2014). The higher sulfur content observed in *G. sulphuraria*-derived LBO (2.9–3.6 wt%) compared to *N. salina*-derived LBO (2.1–2.5 wt%) is attributed in part to the sulfuric acid used in the *G. sulphuraria* growth media (Cheng et al., 2017). No clear trends relating sulfur content to operating conditions were observed.

Elemental distributions (carbon, nitrogen and oxygen) for *G. sulphuraria*-derived HTL products are shown in Fig. 3. Carbon was gradually enriched in LBO with higher reaction temperature; nearly 50% of carbon partitioned into the LBO at 350 °C and 60 min., consistent with the LBO yields. Similar results were observed in the nitrogen distribution, except for the relatively low nitrogen content found at 350 °C and 60 min (Fig. 3(b)). These results imply that more nitrogen-containing compounds partition to the LBO phase under more severe conditions. A different pattern was observed for oxygen distribution (Fig. 3(c)): compared to the moderate conditions, much less oxygen entered the

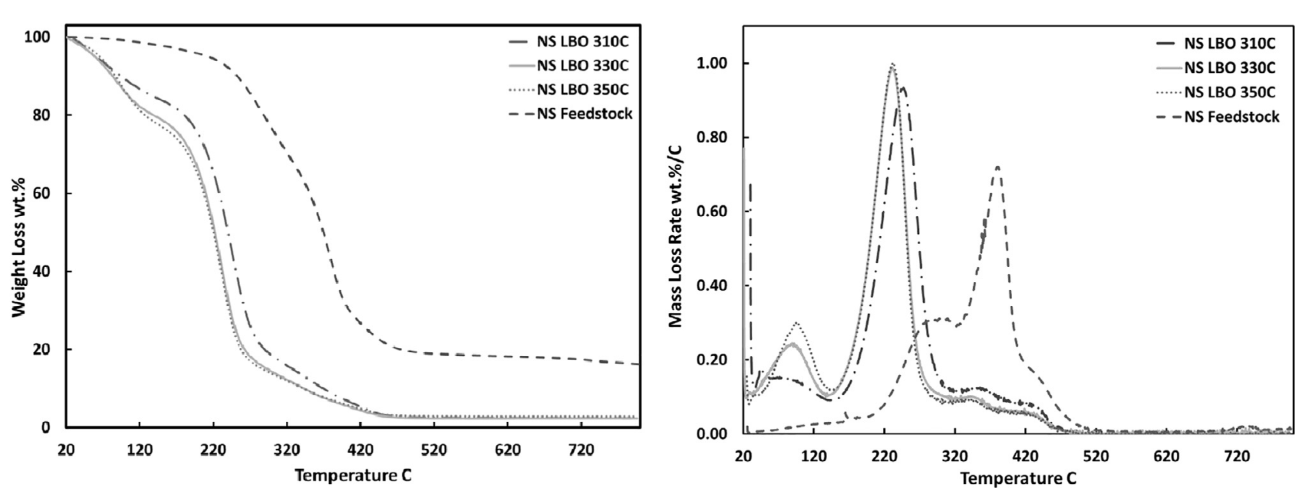

Fig. 2. Thermal decomposition/volatilization (left) and differential thermogravimetric (DTG) curves (right) of 5 wt% *N. salina* and light bio-crude oil (LBO) produced under different HTL temperatures and 60 min. NS = *N. salina*; numbers indicate HTL reaction temperatures.

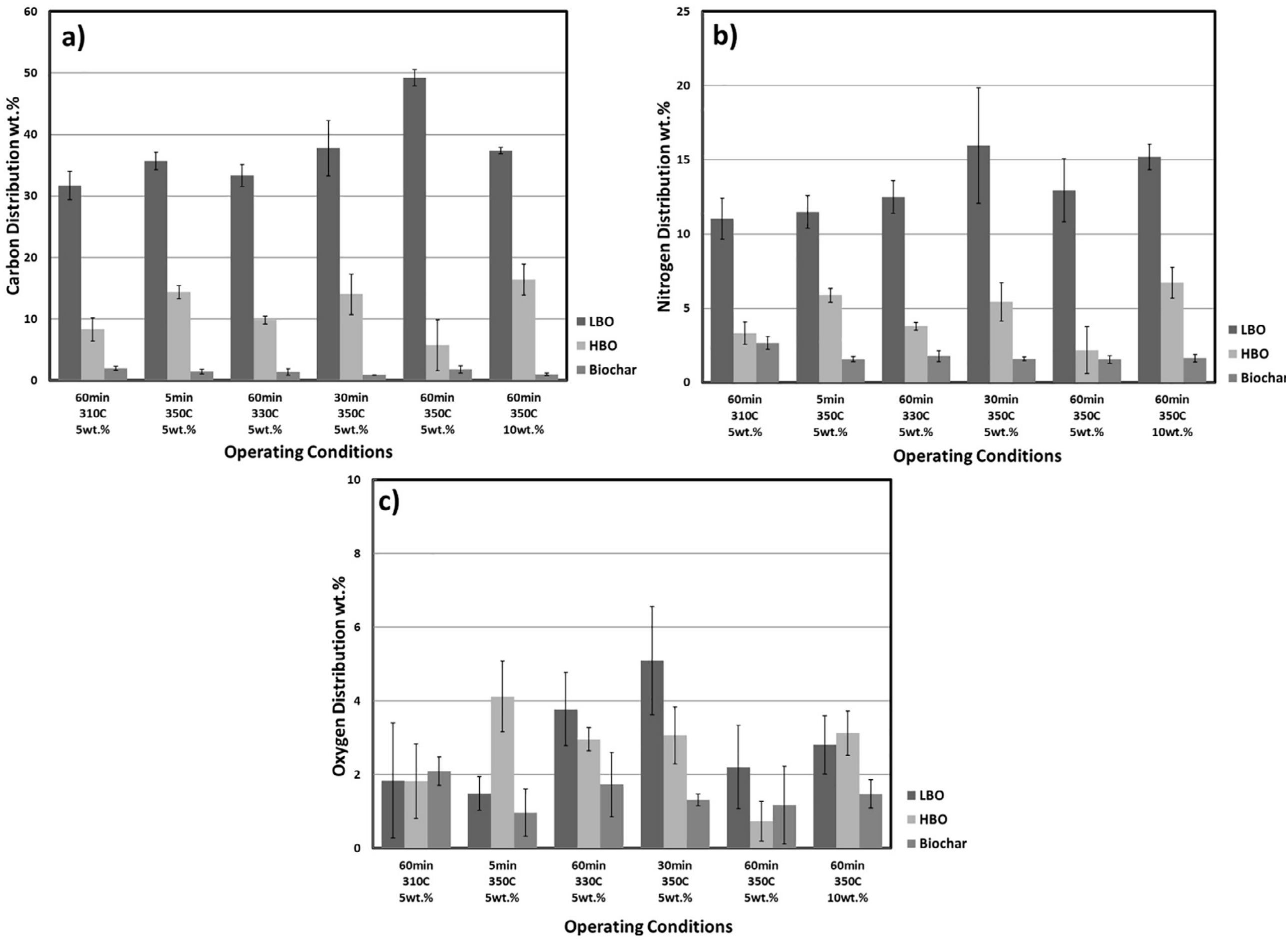

Fig. 3. Elemental distributions of carbon (a), nitrogen (b), and oxygen (c) in *G. sulphuraria*-derived HTL products obtained under different operating conditions. LBO = light bio-crude oil; HBO = heavy bio-crude oil. Error bars represent the standard deviation where n = 2 or 3.

Table 3
Higher heating values (HHV) and energy recovery for light bio-crude oils (LBO) and chars from HTL of *N. salina* and *G. sulphuraria* under different operating conditions. All values reported on a dry weight basis. ECR, energy consumption ratio.

Solid Algal Content wt%	Temp. °C	Time min	Log (R_t)	LBO HHV MJ/kg	LBO Energy Recovery %	LBO ECR	Char HHV[a] MJ/kg	Char Energy Recovery %	Char Ash Content wt%
G. sulphuraria Feedstock				20.5 ± 1.0					
5	310	60	8.03	38.4 ± 6.4	33.8	2.81	6.5 ± 2.7	4.1	85.2[b]
5	350	5	8.55	40.3 ± 0.6	39.5	2.74	8.5 ± 0.5	3.9	87.7[b]
5	330	60	8.62	39.6 ± 0.9	37.8	2.69	9.3 ± 4.2	4.4	85.8 ± 0.6
5	350	30	8.97	39.1 ± 0.3	43.1	2.51	10.9 ± 0.6	5.1	89.7 ± 0.2
5	350	60	9.21	39.5 ± 0.7	52.8	2.05	7.5 ± 1.7	3.4	84.4[b]
10	350	60	9.21	39.9 ± 1.0	42.2	1.23	7.0 ± 1.1	3.3	88.7 ± 0.3
N. salina Feedstock				27.0 ± 0.9					
5	310	5	7.35	40.1 ± 0.9	73.8	0.98	22.4 ± 1.0	5.1	48.3 ± 0.1
5	310	30	7.78	39.3 ± 2.4	75.6	0.96	15.8 ± 0.7	3.2	51.1 ± 0.3
5	310	60	8.03	38.8 ± 1.8	78.1	0.93	19.3 ± 1.6	3.1	53.4[b]
10	310	60	8.03	38.6 ± 0.8	75.0	0.47	16.9 ± 0.2	6.2	47.8 ± 2.7
5	330	60	8.62	39.1 ± 3.1	76.6	1.01	20.2 ± 0.8	3.6	50.0 ± 0.4
5	350	60	9.21	37.4 ± 2.5	55.5	1.48	15.7 ± 0.8	2.8	60.1 ± 0.1

[a] HHV values are the mean of measured values ± one standard deviation for n = 3 for *N. salina* and n = 4 for *G. sulphuraria*. Even with the use of a mineral oil spike to aid combustion, the *G. sulphuraria* char samples did not burn consistently so data should be treated as approximate.
[b] Small sample amount allowed only a single measurement.

LBO phase at 350 °C and 5 min, and 350 °C and 60 min.

Table 3 shows the energy content and energy recovery for bio-crude oils on a reaction ordinate basis. The highest energy content (40.1 MJ/kg) was achieved for *N. salina* under the mildest reaction conditions; this was higher than the HHVs of *Nannochloropsis*-derived bio-crude oils previously (34–39 MJ/kg) (Biller and Ross, 2011; Faeth et al., 2013). As the reaction ordinate increased, HHV decreased for *N. salina*, down to 37.4 MJ/kg for 350 °C and 60 min. These results are consistent with the conversion of lipid-bound fatty acids to free fatty acids at temperatures above 300 °C (Sudasinghe et al., 2015), and dehydration, rearrangement, decomposition, and conversion of saturated bonds into unsaturated bonds—resulting in lower energy contents for oils from

Table 4
Carbon content, pH and electrical conductivity (EC) of aqueous phase fractions from HTL of *N. salina* and *G. sulphuraria* under different operating conditions. ± = one standard deviation where n = 2 for total organic carbon (TOC) and total carbon (TC).

Solid Algal Content wt% [b]	Temp. °C	Time min	Log (R_t)	TOC g/L	TC g/L	pH	EC mS/cm
G. sulphuraria CCMEE 5587.1							
5	310	60	8.03	7.72 ± 0.12	7.91 ± 0.03	8.28	10.0
5	350	5	8.55	9.16 ± 0.13	9.80 ± 0.21	8.82	10.7
5	330	60	8.62	8.48 ± 0.24	8.87 ± 0.18	8.19	9.2
5	350	30	8.97	8.32 ± 0.04	8.92 ± 0.23	8.21	10.2
5	350	60	9.21	8.57 ± 0.1	9.30 ± 0.02	8.47	10.3
10	350	60	9.21	15.02 ± 0.18	16.34 ± 0.1	7.68	21.2
N. salina CCMP 1776							
5	310	5	7.35	6.10 ± 0.03	6.44 ± 0.03	9.01	6.1
5	310	30	7.78	6.04 ± 0.12	6.50 ± 0.15	8.33	6.3
5	310	60	8.03	6.32 ± 0.05	6.44 ± 0.01	8.65	6.6
10	310	60	8.03	10.12 ± 0.02	10.96 ± 0.2	8.89	12.6
5	330	60	8.62	5.84 ± 0.22	6.62 ± 0.08	8.88	6.1
5	350	60	9.21	6.07 ± 0.05	6.83 ± 0.42	8.67	6.6

higher reaction temperatures, most notably at 350 °C. The small increase in bio-crude oil HHV at 330 °C may be attributed to incorporation of carbohydrate- and protein-derived compounds with moderately high energy contents into the organic phase from the aqueous phase. For *G. sulphuraria,* the bio-crude oil energy content values ranged from 38.2 to 40.3 MJ/kg, and did not show any trends in relation to reaction conditions.

For *N. salina*, energy recoveries in the LBO ranged from 74% to 78% for all reaction conditions tested—recoveries higher than those in previous studies (Barreiro et al., 2015a; Brown et al., 2010), except for the most severe condition at 350 °C (log (R_t) = 9.21), when the energy recovery was only 55.5%. For *G. sulphuraria*, energy recoveries were much lower (34–53%), primarily due to the substantially lower yields as the energy contents of the bio-crude oils were comparable to those of *N. salina*. Energy recoveries increased with reaction ordinate, indicating that most energy-rich fractions (e.g. protein and carbohydrate) of *G. sulphuraria* biomass require more severe conditions to be converted than those in *N. salina*. Notably, the increase from 5 to 10 wt% solid algae contents did not appear to impact the energy recovery for *N. salina* substantially (78% vs. 75%), whereas the energy recovery for *G. sulphuraria* was 10% lower at the higher solids loading, and was 9% lower for 30 min compared to 60 min, suggesting that heat and mass transfer limitations may play more of a role in the energy recovery for *G. sulphuraria* than for *N. salina*, possibly due to the larger particle sizes of *G. sulphuraria*.

Calculated energy consumption ratios (ECR) were much lower for HTL of *N. salina* (0.47–1.48) than for HTL of *G. sulphuraria* (1.23–2.81) (Table 3). This indicates that, for the assumptions made here, more energy would be needed to convert *G. sulphuraria* biomass than could be obtained during combustion of its LBO. Differences in ECR between algae species and between HTL reaction conditions are influenced

Table 6
Total elemental content of algal biomass feedstock and HTL products by microwave acid digestion (except aqueous phase) and ICP quantification. Biomass composition is the average of two samples. Blank cells represent a non-detect.

Element	Biomass mg/kg	LBO mg/kg	HBO mg/kg	Char mg/kg	Aqueous phase mg/kg
N. salina (5 wt%, 310 °C, 60 min, log (R_t) = 8.03)					
Na	12,215			1,685	515
K	11,585		156	1,013	567
P	5814	200	1172	92,240	5
S	5441	1,204	3376	4,541	170
Mg	3640	76	377	39,300	5
Ca	1764	184	1719	124,300	4
Fe	208	169	3602	6671	1
Al	118	129	101	1540	0.5
Mn	41	3	29	770	
Zn	32	13	99	199	
Sr	23	6	21	1642	
Cr		7	82	758	
Mo			41	91	
Ni		13	168	473	
G. sulphuraria (5 wt%, 350 °C, 60 min, log (R_t) = 9.21)					
P	22,195	63	121	172,100	172
Al	11,960	35	426	127,100	1
S	11,595	10,660	7,096	943	229
K	7378			19,850	303
Mg	1926		80	23,820	1
Fe	1627	117	1208	14,280	
Na	553				30
Ca	356			877	4
Cr	74	4	31	649	
Zn	54	9	78	296	
Mn	44		3	425	
Ba	44	1		357	
Mo	16		106	41	
Ni	3	13	96	93	

primarily by the parameters in the denominator of the equation (Eq. (2) since the reaction conditions were similar across the tested parameters while the bio-crude oil yields and energy contents varied substantially. Because the yields of *N. salina* LBO were almost twice those of *G. sulphuraria*, the ECR of *N. salina* HTL is almost half of those of *G. sulphuraria* HTL. With regards to solid algae content, HTL of 10 wt% algal dry matter gave lower ECR values (0.47 for *N. salina* and 1.23 for *G. sulphuraria*) than for HTL of 5 wt% algal dry mater (0.93 for *N. salina* and 2.05 for *G. sulphuraria*). The lower ECR for higher algal content is directly related to higher bio-crude oil productivity and lower heat capacity of dry algal biomass. Since the bio-crude oil yields and energy contents did not vary much between 5 and 10 wt% algal dry matter, higher solids loadings are desirable from an energy efficiency perspective. In continuous flow reactors, the solids loadings of algae feedstock are limited by heat transfer, clogging, and fouling issues downstream (Jazrawi et al., 2013). As this study was intended to inform continuous flow reactor development, solids loadings were selected at or below 10 wt%.

Based on energy analysis of the HTL process, ECR values of *G.*

Table 5
Elemental composition of char and heavy bio-crude oil (HBO) fractions from HTL of *G. sulphuraria* under different operating conditions. All values on a dry weight basis.

Solid Algal Content wt%	Temp. °C	Time min	Log (R_t)	Char				HBO					
				C %	H %	N %	S %	C %	H %	N %	S %	HHV MJ/kg	Energy Recovery %
5	310	60	8.03	6.7 ± 0.1	1.4 ± 0.2	1.9 ± 0.1	0.7 ± 0.1	73.8 ± 4.6	8.5 ± 0.8	6.3 ± 0.3	2.3 ± 0.3	34.9	8.6
5	350	5	8.55	6.7 ± 1.7	0.9 ± 0.1	1.6 ± 0.1	0.5 ± 0.1	71.7 ± 2.4	8.1 ± 0.3	6.2 ± 0.2	2.2 ± 0.2	33.5	14.5
5	330	60	8.62	6.1 ± 1.9	1.2 ± 0.1	1.7 ± 0.1	0.7 ± 0.2	71.7 ± 0.4	8.1 ± 0.2	5.9 ± 0.0	2.0 ± 0.2	33.4	9.9
5	350	30	8.97	4.0 ± 0.1	0.8 ± 0.1	1.6 ± 0.1	0.5 ± 0.1	74.0 ± 0.3	8.4 ± 0.1	6.1 ± 0.0	2.3 ± 0.2	34.9	14.2
5	350	60	9.21	8.6 ± 2.8	1.5 ± 0.3	1.6 ± 0.2	0.8 ± 0.1	76.8 ± 0.3	8.7 ± 0.3	6.2 ± 0.0	2.6 ± 0.6	36.6	5.9
10	350	60	9.21	4.5 ± 0.7	0.9 ± 0.0	1.6 ± 0.1	0.5 ± 0.1	75.1 ± 0.7	8.3 ± 0.2	6.5 ± 0.1	1.9 ± 0.1	35.2	16.6

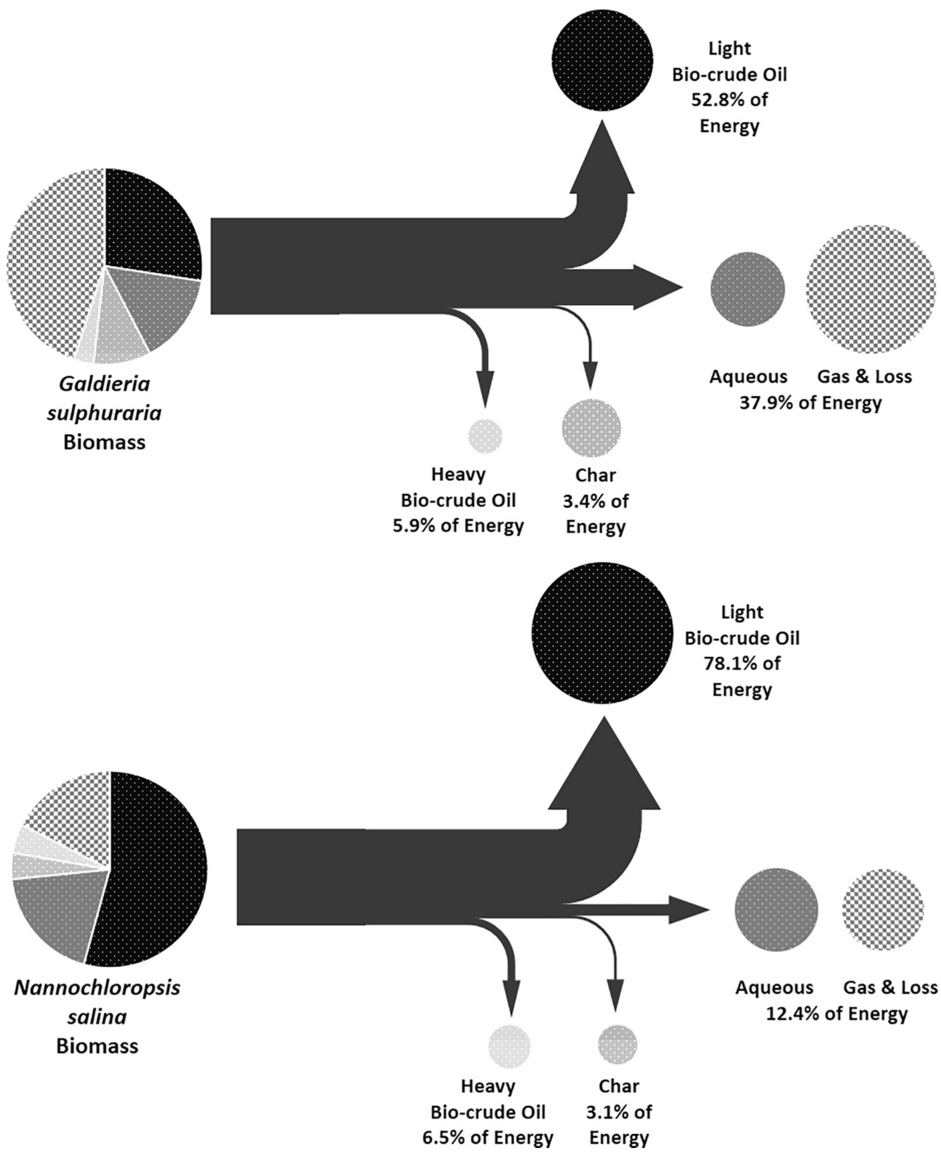

Fig. 4. Energy flows in HTL of 5 wt% *G. sulphuraria* at 350 °C for 60 min and of 5 wt% *N. salina* at 310 °C for 60 min. Arrow thickness represents the value of energy recovery for each HTL products. Circle area indicates the yield of each HTL product.

sulphuraria HTL were higher than 1. However, *G. sulphuraria* is not intended as a fuel crop but as a heterotrophic strain for wastewater treatment as an alternative to the energy-intensive activated sludge process (Henkanatte-Gedara et al., 2015; Henkanatte-Gedara et al., 2017). The high ECR in the HTL process may be offset by energy savings in the wastewater treatment process if an overall energy balance is performed for the integrated wastewater treatment-HTL process. Engineering efforts to improve ECR are still needed, such as increasing bio-oil yield and HHV via pretreating feedstock and modifying HTL process conditions, increasing algal solids loadings, integrating various heat sources from other processes, and modifying reactor configurations.

3.5. Aqueous phase characteristics

Compositional data for the aqueous phase products are shown in Table 4. For *G. sulphuraria*, total carbon (TC) contents ranged from 7.9 to 16.3 g/L, with > 90% of that carbon being organic. The aqueous phase from conversion of 10 wt% algae contained nearly twice the amount of TC and EC than that from conversion of 5 wt% algae, indicating that the concentration scales with the solids loading. Solution pH values ranged from 7.7 to 8.8, with a slightly positive correlation with total organic carbon. The slightly alkaline pH values are speculated to be caused by the high protein content in *G. sulphuraria* feedstock contributing hydrophilic amines into the aqueous phase during HTL. The aqueous phase from conversion of *N. salina* followed the same pattern related to solids loading and fraction of organic carbon, albeit with lower overall amounts: TC ranged from 5.8 to 10.1 g/L and EC ranged from 6.1 to 12.6 mS/cm. The pH was higher (8.3–9.0), which could not be explained by high protein content. Rather, the alkaline pH values are attributed to higher amounts of alkaline and alkaline earth metal salts (e.g. Na, Mg, Ca, and K) (Table 6). Reaction time and temperature did not show any clear trends in aqueous phase water chemistry or carbon partitioning.

3.6. HBO and char characteristics

The limited sample size and high viscosity of the HBO samples limited the ability to characterize those samples. Table 5 shows the CHNS content of the HBO from *G. sulphuraria*. Carbon and hydrogen contents were lower than those for LBO (71–77 wt% vs. 74–80 wt%, and 8.1–8.7 wt% vs. 10.0–10.7 wt%), which resulted in a higher calculated oxygen content for the HBO, which is consistent with the higher number of oxygenated compounds in HBO (Cheng et al., 2017). Estimations of the HBO HHV using elemental content correlations (Channiwala and Parikh, 2002) ranged from 33.4 MJ/kg to 36.7 MJ/kg, representing approximately 6–17% of the energy in the *G. sulphuraria* biomass (Table 5). The energy recovery of HBO, comparable to that of LBO, means that considerable energy could be gained from HBO for biofuel production via upgrading and mixing with LBO.

Compositional data and properties for the chars are shown in Tables 3 and 5. The energy contents of the chars ranged from 6.5 to 10.9 MJ/kg and from 15.7 to 22.4 MJ/kg, representing 3.3–5.1% and 2.8–6.2% of the energy content in the biomass for *G. sulphuraria* and *N. salina*, respectively. Both chars were high in ash, 85–90 wt% for *G. sulphuraria* and 47–60 wt% for *N. salina*, which creates a potential for fouling in continuous flow reactor systems and may require acid pretreatment to remove ash from the feedstock.

In Fig. 4, at the conditions of the highest LBO yields, *N. salina* HTL partitioned algal biomass energy as 78% to LBO, 7% to HBO, 3% to char, and the remaining 12% between the aqueous phase and gases. *G. sulphuraria* HTL partitioned algal biomass energy as 53% to LBO, 6% to HBO, 3% to char, and 38% to the aqueous phase and gases. The most substantial difference in energy partitioning between the two algal species is among the aqueous, the gaseous, and the LBO phases, with more energy partitioning into the oil phase for *N. salina* compared to *G. sulphuraria*—as would be expected from the greater amount of heteroatoms in the protein- and carbohydrate-derived compounds from *G. sulphuraria*, giving those compounds higher polarity than the lipid-derived compounds from *N. salina* (Cheng et al., 2017). Therefore, facilitating the organics transfer from aqueous and gaseous to oily phase plays a primary role on the energy recovery from low-lipid high-protein algae.

Table 6 shows the acid digestion inorganic elemental analysis of the biomass and HTL product fractions. Most of the inorganic elements present are microbial macro and micronutrients, with trace amounts of other metals. *G. sulphuraria* feedstock and products contained a substantial amount of aluminum. This is explained by the acidic growth environment and the use of aluminum in the growth chamber components (i.e. the paddlewheels), where corrosion was observed on the aluminum surfaces. Water-soluble salts (Na and K) tended to partition into the aqueous phase while less water-soluble elements (Ca, Mg, P, most metals) concentrated in the char fraction. The sulfur partitioned between all of the fractions, which supports the presence of sulfur in the LBO (Table 1). These results are important if nutrients are to be recovered from the aqueous and char fractions, and for oil components that may sinter/foul catalysts during downstream processing.

4. Conclusions

G. sulphuraria-derived bio-crude oils required more severe conditions than for *N. salina*, as protein conversion into oil-phase compounds requires more energy. 31 wt% of the dry mass and 53% of the energy from *G. sulphuraria* were recovered as bio-crude oil. The partitioning of organic products between the aqueous phase and the solvent-extracted phase had a substantial impact on mass and energy recoveries. For both algal species, shorter reaction times and higher solids loadings led to similar yields and energy contents of bio-crude oils, and lower energy consumption ratios, therefore, such conditions should be adopted in continuous flow reactor systems.

Acknowledgements

The authors would like to acknowledge funding from the National Science Foundation “ReNUWIt” Engineering Research Center (#1028968), the National Science Foundation New Mexico EPSCOR Research Infrastructure Improvement grant “Energize New Mexico” (#1031346), the U.S. Department of Energy Regional Algal Fuels Testbed Partnership (#DE-EE0006269), and the NMSU Ed & Harold Foreman Endowed Chair. The authors would also like to acknowledge assistance from members of the Holguin, VanVoohries, Boeing, Khandan, and Brewer research groups during algae production, harvesting, and characterization, and HTL reactor operation and product characterization.

References

Barreiro, D.L., Riede, S., Hornung, U., Kruse, A., Prins, W., 2015a. Hydrothermal liquefaction of microalgae: effect on the product yields of the addition of an organic solvent to separate the aqueous phase and the biocrude oil. Algal Res. 12, 206–212.
Barreiro, D.L., Zamalloa, C., Boon, N., Vyverman, W., Ronsse, F., Brilman, W., Prins, W., 2013. Influence of strain-specific parameters on hydrothermal liquefaction of microalgae. Bioresour. Technol. 146, 463–471.
Barreiro, D.L.P., Gómez, B.R., Hornung, U., Kruse, A., Prins, W., 2015b. Hydrothermal liquefaction of microalgae in a continuous stirred-tank reactor. Energy Fuels 29 (10), 6422–6432.
Biddy, M., Davis, R., Jones, S., Zhu, Y., 2013. Whole algae hydrothermal liquefaction technology pathway. National Renewable Energy Laboratory Golden.
Biller, P., Ross, A.B., 2011. Potential yields and properties of oil from the hydrothermal liquefaction of microalgae with different biochemical content. Bioresour. Technol. 102 (1), 215–225.
Biller, P., Sharma, B.K., Kunwar, B., Ross, A.B., 2015. Hydroprocessing of bio-crude from continuous hydrothermal liquefaction of microalgae. Fuel 159, 197–205.
Brown, T.M., Duan, P., Savage, P.E., 2010. Hydrothermal liquefaction and gasification of Nannochloropsis sp. Energy Fuels 24 (6), 3639–3646.
Campos, H., Boeing, W.J., Dungan, B.N., Schaub, T., 2014. Cultivating the marine microalga Nannochloropsis salina under various nitrogen sources: effect on biovolume yields, lipid content and composition, and invasive organisms. Biomass Bioenergy 66 (Suppl. C), 301–307.
Chakraborty, M., Miao, C., McDonald, A., Chen, S., 2012. Concomitant extraction of bio-oil and value added polysaccharides from Chlorella sorokiniana using a unique sequential hydrothermal extraction technology. Fuel 95, 63–70.
Channiwala, S.A., Parikh, P.P., 2002. A unified correlation for estimating HHV of solid, liquid and gaseous fuels. Fuel 81 (8), 1051–1063.
Chen, Y.-Q., Wang, N., Zhang, P., Zhou, H., Qu, L.-H., 2002. Molecular evidence identifies bloom-forming Phaeocystis (Prymnesiophyta) from coastal waters of southeast China as Phaeocystis globosa. Biochem. Syst. Ecol. 30 (1), 15–22.
Cheng, F., Cui, Z., Chen, L., Jarvis, J., Paz, N., Schaub, T., Nirmalakhandan, N., Brewer, C.E., 2017. Hydrothermal liquefaction of high-and low-lipid algae: bio-crude oil chemistry. Appl. Energy 206, 278–292.
Chretiennot-Dinet, M.-J., Vaulot, D., Galois, R., Spano, A.-M., Robert, R., 1991. Analysis of larval oyster grazing by flow cytometry. J. Shellfish Res. 10 (2), 457–463.
Elliott, D.C., Hart, T.R., Neuenschwander, G.G., Rotness, L.J., Roesijadi, G., Zacher, A.H., Magnuson, J.K., 2013a. Hydrothermal processing of macroalgal feedstocks in continuous-flow reactors. ACS Sustain. Chem. Eng. 2 (2), 207–215.
Elliott, D.C., Hart, T.R., Schmidt, A.J., Neuenschwander, G.G., Rotness, L.J., Olarte, M.V., Zacher, A.H., Albrecht, K.O., Hallen, R.T., Holladay, J.E., 2013b. Process development for hydrothermal liquefaction of algae feedstocks in a continuous-flow reactor. Algal Res. 2 (4), 445–454.
Faeth, J.L., Valdez, P.J., Savage, P.E., 2013. Fast hydrothermal liquefaction of Nannochloropsis sp. to produce biocrude. Energy Fuels 27 (3), 1391–1398.
Hames, B., Scarlata, C., Sluiter, A., 2008. Determination of Protein Content in Biomass. National Renewable Energy Laboratory.
Henkanatte-Gedara, S.M., Selvaratnam, T., Caskan, N., Nirmalakhandan, N., 2015. Algal-based, single-step treatment of urban wastewaters. Biores. Tech. 189, 273–278.
Henkanatte-Gedara, S.M., Selvaratnam, T., Karbakhshravari, M., Nirmalakhandan, N., 2017. Removal of dissolved organic carbon and nutrients from urban wastewaters by *Galdieria sulphuraria*: laboratory to field scale demonstration. Algal Res. 24, 450–456.
Hu, E., Xu, Y., Hu, X., Pan, L., Jiang, S., 2012. Corrosion behaviors of metals in biodiesel from rapeseed oil and methanol. Renew. Energy 37 (1), 371–378.
Jazrawi, C., Biller, P., Ross, A.B., Montoya, A., Maschmeyer, T., Haynes, B.S., 2013. Pilot plant testing of continuous hydrothermal liquefaction of microalgae. Algal Res. 2 (3), 268–277.
Jena, U., Das, K., Kastner, J., 2011. Effect of operating conditions of thermochemical liquefaction on biocrude production from Spirulina platensis. Bioresour. Technol. 102 (10), 6221–6229.
Leow, S., Witter, J.R., Vardon, D.R., Sharma, B.K., Guest, J.S., Strathmann, T.J., 2015. Prediction of microalgae hydrothermal liquefaction products from feedstock biochemical composition. Green Chem. 17 (6), 3584–3599.
Li, H., Liu, Z., Zhang, Y., Li, B., Lu, H., Duan, N., Liu, M., Zhu, Z., Si, B., 2014. Conversion efficiency and oil quality of low-lipid high-protein and high-lipid low-protein microalgae via hydrothermal liquefaction. Bioresour. Technol. 154, 322–329.
Minowa, T., Kondo, T., Sudirjo, S.T., 1998. Thermochemical liquefaction of Indonesian biomass residues. Biomass Bioenergy 14 (5), 517–524.
Minowa, T., Yokoyama, S.-Y., Kishimoto, M., Okakura, T., 1995. Oil production from algal cells of Dunaliella tertiolecta by direct thermochemical liquefaction. Fuel 74 (12), 1735–1738.
Overend, R.P., Chornet, E., Gascoigne, J., 1987. Fractionation of lignocellulosics by steam-aqueous pretreatments [and discussion]. Philos. Trans. R. Soc. London, Ser. A 321 (1561), 523–536.
Reddy, H.K., Muppaneni, T., Ponnusamy, S., Sudasinghe, N., Pegallapati, A., Selvaratnam,

T., Seger, M., Dungan, B., Nirmalakhandan, N., Schaub, T., 2016. Temperature effect on hydrothermal liquefaction of Nannochloropsis gaditana and Chlorella sp. Appl. Energy 165, 943–951.

Reeb, V., Bhattacharya, D., 2010. The Thermo-Acidophilic Cyanidiophyceae (Cyanidiales). In: Seckbach, J. (Ed.), Red Algae in the Genomic Age. Springer, D.J. Chapman, pp. 409–426.

Richter, H., Howard, J.B., 2000. Formation of polycyclic aromatic hydrocarbons and their growth to soot—a review of chemical reaction pathways. Progr. Energy Combust. Sci. 26 (4), 565–608.

Rodolfi, L., Chini Zittelli, G., Bassi, N., Padovani, G., Biondi, N., Bonini, G., Tredici, M.R., 2009. Microalgae for oil: strain selection, induction of lipid synthesis and outdoor mass cultivation in a low-cost photobioreactor. Biotechnol. Bioeng. 102 (1), 100–112.

Schönknecht, G., Chen, W.-H., Ternes, C.M., Barbier, G.G., Shrestha, R.P., Stanke, M., Bräutigam, A., Baker, B.J., Banfield, J.F., Garavito, R.M., 2013. Gene transfer from bacteria and archaea facilitated evolution of an extremophilic eukaryote. Science 339 (6124), 1207–1210.

Selvaratnam, T., Pegallapati, A., Montelya, F., Rodriguez, G., Nirmalakhandan, N., Lammers, P.J., Van Voorhies, W., 2015a. Feasibility of algal systems for sustainable wastewater treatment. Renew. Energy 82, 71–76.

Selvaratnam, T., Reddy, H., Muppaneni, T., Holguin, F., Nirmalakhandan, N., Lammers, P.J., Deng, S., 2015b. Optimizing energy yields from nutrient recycling using sequential hydrothermal liquefaction with Galdieria sulphuraria. Algal Res. 12, 74–79.

Simpson, A.J., Zang, X., Kramer, R., Hatcher, P.G., 2003. New insights on the structure of algaenan from Botryoccocus braunii race A and its hexane insoluble botryals based on multidimensional NMR spectroscopy and electrospray–mass spectrometry techniques. Phytochemistry 62 (5), 783–796.

Speight, J.G., 2014. The Chemistry and Technology of Petroleum, Fifth ed. CRC Press, Boca Raton, FL.

Sudasinghe, N., Reddy, H., Csakan, N., Deng, S., Lammers, P., Schaub, T., 2015. Temperature-dependent lipid conversion and nonlipid composition of microalgal hydrothermal liquefaction oils monitored by Fourier transform ion cyclotron resonance mass spectrometry. BioEnergy Res. 8 (4), 1962–1972.

Tian, C., Liu, Z., Zhang, Y., Li, B., Cao, W., Lu, H., Duan, N., Zhang, L., Zhang, T., 2015. Hydrothermal liquefaction of harvested high-ash low-lipid algal biomass from Dianchi Lake: effects of operational parameters and relations of products. Bioresour. Technol. 184 (Suppl. C), 336–343.

Toplin, J., Norris, T., Lehr, C., McDermott, T., Castenholz, R., 2008. Biogeographic and phylogenetic diversity of thermoacidophilic cyanidiales in Yellowstone National Park, Japan, and New Zealand. Appl. Environ. Microbiol. 74 (9), 2822–2833.

Valdez, P.J., Tocco, V.J., Savage, P.E., 2014. A general kinetic model for the hydrothermal liquefaction of microalgae. Bioresour. Technol. 163, 123–127.

Wychen, S.V., Laurens, L.M.L., 2013a. Determination of Total Carbohydrates in Algal Biomass. National Renewable Energy Laboratory.

Wychen, S.V., Laurens, L.M.L., 2013b. Determination of Total Solids and Ash in Algal Biomass. National Renewable Energy Laboratory.

Wychen, S.V., Ramirez, K., Laurens, L.M.L., 2013. Determination of Total Lipids as Fatty Acid Methyl Esters (FAME) by in situ Transesterification. National Renewable Energy Laboratory.

Xu, D., Savage, P.E., 2014. Characterization of biocrudes recovered with and without solvent after hydrothermal liquefaction of algae. Algal Research 6, 1–7.